ELSEVIER

Modeling the dynamics of double-diffusive scalar fields at various stability conditions

K. Hanjalić* and R. Musemić†

Faculty of Applied Physics,* Delft University of Technology, Delft, The Netherlands, and Mašinski fakultet,† University of Sarajevo, Bosnia and Hercegovina

This paper presents some results of mathematical modeling and numerical computation of the dynamics of the temperature and concentration fields in simulated salt-gradient solar ponds, which are commonly used for collection and long-term storage of solar- and otherwise-generated heat. The pond has been treated as a two-layer, double-diffusive system, infinite in the horizontal plane, initially stably stratified by downward salinity gradient and with a uniform (or stably stratified) temperature distribution, which has been subjected to stratification disturbance by supplying heat from the bottom. The method of simulation employs a two-equation model of turbulence with variable turbulent Prandtl–Schmidt numbers, modified to account for thermal and mass buoyancy. The predictions obtained agree well with several sets of experimental data available in the literature.

Keywords: double diffusion; turbulence modeling; solar ponds

Introduction

Two-layer, nonconvective solar salt ponds represent a convenient and efficient way for collection and long-term storage of the available heat in solar energy systems and in other types of storage space heating, as well as in process engineering and energy conversion technologies. Their storage performance is based on the separation of the upper cold fresh water from the hot salty layer beneath it by a natural diffusive (molecular) interface, which prevents upward loss of accumulated heat from the bottom layer. Hence, the characteristics of the thermal resistance of the diffusive interface and its stability, govern, to a large extent, the salt pond operation.

A solar salt pond is a typical example of a double-diffusive system, found in nature (oceans and salty lakes) and in many areas of engineering, in which a strong density stratification dominates the transport processes (metal solidification and crystal growth, heavy gas storage, handling, etc.). The stratification is usually expressed in terms of density increment $\Delta\rho = \Delta\rho_T + \Delta\rho_s = \rho_0(-\alpha\,\Delta T + \beta\,\Delta S)$, where $\alpha = -1/\rho_0(\partial\rho/\partial T)_S$ and $\beta = 1/\rho_0(\partial\rho/\partial S)_T$ denote the volume expansion coefficients caused by unit temperature and concentration changes, respectively. The double-diffusive systems can be characterized by two or more layers of fluid of different densities separated by a (molecular) diffusive interface, as indicated in Figure 1. The bottom layer is well mixed because of the unstable stratification usually caused by direct or indirect (e.g., solar radiation) heating of the pond bottom. Unstable stratification generates turbulence, which promotes intensive mixing and local upward convection in the lower layer, which tends to spread upwards working against the usually stable concentration gradient. Depending on the ratio of the bottom heat flux and concentration gradient, the lower mixed layer can either overtake the whole fluid, or remain trapped below the diffusive interface. The upper layer may also be well mixed because of convection or mechanical (e.g., wind shear) turbulence production locally or elsewhere in the layer (Figure 1b). Such situations are found in oceans, where several turbulent, well-mixed, layers may exist, separated one from another by sharp interfaces through which intensive transport of heat and salt occurs (Turner 1965). However, in solar ponds and in many other cases, the upper fluid remains nonturbulent and often stagnant, dominated by molecular transport (Figure 1a).

In the literature there are simple theories (e.g., Turner 1965; Fernando 1989) that correlate the principal integral properties of the double-diffusive systems (the criteria for the establishment of the double-layer system and its stability; the dynamics of bottom mixed-layer growth, etc.). However, none of these theories gives the possibility to predict details of the temperature and concentration fields and their interaction.

The approach described here is based on the modeled differential equations for turbulent fluxes of heat and species, which, in conjunction with mean momentum, enthalpy, and concentration equations enables prediction of velocity, temperature, and concentration fields under different stability conditions, and from which all relevant integral properties can be deduced. A simplified form of turbulence closure, truncated to a common form of two-equation model, but modified to account for thermal and mass buoyancy, produced results that are in acceptable agreement with experimental data of several authors. The paper presents the basic theory and compares a range of predicted results with experimental data.

Address reprint requests to Prof. K. Hanjalić, Faculty of Applied Physics, Delft University of Technology, Lorentzweg 1, 2628 CJ Delft, The Netherlands.

Received 6 May 1996; accepted 26 November 1996

Int. J. Heat and Fluid Flow 18:360–367, 1997

655 Avenue of the Americas, New York, NY 10010

0142-727X/97/$17.00
PII S0142-727X(97)00018-0

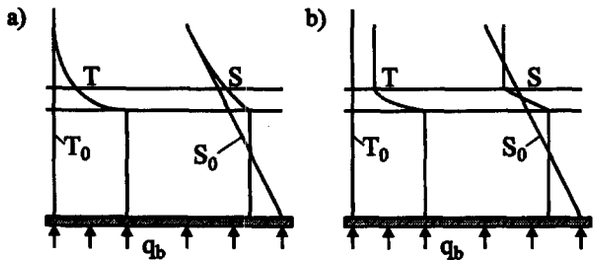

Figure 1 Schematic of a two-layer salt-stratified pond heated from below; a, upper layer unmixed; b, both layers well-mixed

A second-moment closure for double-diffusive systems: the rationale

Although integral relationships can be useful for estimating the basic properties of double-diffusive systems, the mathematical modeling and numerical computations of field properties (temperature, concentration, and density fields) in *differential* form yields much more accurate and detailed predictions of all relevant parameters. It is known that models of turbulence of various levels of complexity have been successful in predicting turbulent flows and transport phenomena in different situations, especially if the process is dominated by shear. However, in the case of buoyancy-driven turbulent motion, there are several phenomena originating from the strong coupling and mutual interaction between the temperature, concentration and velocity fields that must be considered. A particular challenge arises in modeling the turbulent transport in mixed layers such as those found in solar ponds, where the mean temperature and concentration fields are almost uniform. Here, the conventional gradient hypothesis, by which the turbulent fluxes are modeled in terms of the mean property gradients, fails to produce sensible results, because it yields very small or negligible vertical turbulent fluxes. It should be pointed out that these fluxes, generated by buoyancy, are significant in magnitude, representing the major cause of upward turbulent convection and mixing so that the almost uniform temperature and concentration distributions are *the consequence*, not the cause, of the vertical turbulent fluxes. A proper mathematical representation should employ a higher-order modeling approach, such as implied by differential stress/flux turbulence models or, at least, some simplified variant that gives a more general representation of the turbulent diffusion than is provided by simple gradient hypothesis. Another important feature of the double-diffusive systems is a significant influence of molecular interactions within the diffusive interface and in its vicinity, regardless of the intensity of turbulence in the mixed layers. This makes it necessary to include the molecular effects in all turbulence equations.

In the absence of a significant mean fluid motion and with the assumption that the transport of all properties is one-dimensional (in vertical direction, denoted by z), the mean energy (in terms of temperature T), and mean concentration (S), equations can be written

$$\rho \frac{\partial T}{\partial t} = \frac{\partial}{\partial z}\left(\frac{\mu}{\sigma_T}\frac{\partial T}{\partial z}\right) - \frac{\partial(\rho\overline{w\theta})}{\partial z} \tag{1}$$

Notation

B_S	concentration buoyancy parameter, $g\beta(k/\varepsilon)^2\,\partial S/\partial z$
B_T	thermal buoyancy parameter, $g\alpha(k/\varepsilon)^2\,\partial T/\partial z$
C	empirical coefficients in the turbulence model
f_μ, f_ε	damping functions in the turbulence model
g_i	gravitation vector
h	layer thickness
k	kinetic energy of turbulence
Pr	Prandtl number, ν/α
R	scalar/mechanical turbulence time scale ratio, $\overline{\theta^2}\varepsilon/2k\varepsilon_\theta = \overline{s^2}\varepsilon/2k\varepsilon_s$
Ra	Rayleigh number
R_s	Turner's stability parameter, $\beta\,\Delta S/\alpha\,\Delta T$
Re_t	turbulence Reynolds number, $k^2/\nu\varepsilon$
s	turbulent fluctuation of salt concentration
$\overline{s^2}$	variance of turbulent concentration fluctuations
$\overline{su_i}$	turbulent mass flux vector
S	mean salt concentration
t	time coordinate
T	mean temperature
u_i	turbulent fluctuation of the velocity vector
U_i	mean velocity vector
$\overline{u_iu_j}$	turbulent stress tensor
w	vertical velocity fluctuations
x_i	space coordinates
X	stability parameter, $\alpha q_b/\lambda\beta(\partial S/\partial z)$
z	vertical coordinate directed upward

Greek

α	thermal expansion factor, $-(1/\rho_0)(\partial\rho/\partial T)_S$
β	concentration expansion factor, $(1/\rho_0)(\partial\rho/\partial S)_T$
ε	dissipation rate of the turbulence kinetic energy k
ε_θ	dissipation rate of the temperature variance $\overline{\theta^2}$
ε_s	dissipation rate of the concentration variance $\overline{s^2}$
ε_{θ_i}	dissipation rate of the turbulent heat flux $\overline{\theta u_i}$
ε_{s_i}	dissipation rate of the turbulent concentration flux $\overline{su_i}$
ε_{θ_s}	dissipation rate of the scalar cross-correlation $\overline{\theta s}$
$\tilde{\varepsilon}, \tilde{\varepsilon}_\theta$	homogeneous parts of ε and ε_θ
$\overline{\theta u_i}$	turbulent heat flux vector
$\overline{\theta s}$	single-point correlation of temperature and concentration fluctuations
$\overline{\theta^2}$	temperature variance
λ	thermal conductivity
μ	dynamic viscosity
ν	kinematic viscosity
ρ	fluid density
σ	turbulent Prandtl–Schmidt number for a turbulent property
τ	time
Φ	empirical coefficients in the turbulence model
ϕ	general notation for the fluctuation of a scalar
ψ	general notation for the fluctuation of a scalar

Subscripts

0	characteristic, reference value
eff	effective
m	mixed layer
S	concentration field
t	turbulent
T	thermal field

$$\rho \frac{\partial S}{\partial t} = \frac{\partial}{\partial z}\left(\frac{\mu}{\sigma_S}\frac{\partial S}{\partial z}\right) - \frac{\partial(\rho\overline{ws})}{\partial z} \tag{2}$$

Second-moment closure formally entails the solution of the differential transport equations for the turbulent fluxes of heat and species $\overline{w\theta}$ and $\overline{ws}$, respectively. For a unidirectional transport in the vertical direction and under the assumption that the vertical normal stress component $\overline{w^2}$ is proportional to be turbulence kinetic energy, the flux equations reduce to:

$$\rho \frac{\partial \overline{w\theta}}{\partial t} = \frac{\partial}{\partial z}\left(\frac{\mu_{ef}}{\sigma_{\overline{w\theta}}}\frac{\partial \overline{w\theta}}{\chi z}\right) + (1 - C_{T_2})(\rho g\alpha\overline{\theta^2} - \rho g\beta\overline{\theta s}) - \frac{1}{2}\rho k\frac{\partial T}{\partial z} - C_{T_1}\rho\frac{\varepsilon}{k}\overline{w\theta} \tag{3}$$

$$\rho \frac{\partial \overline{ws}}{\partial t} = \frac{\partial}{\partial z}\left(\frac{\mu_{ef}}{\sigma_{\overline{ws}}}\frac{\partial \overline{ws}}{\partial z}\right) + (1 - C_{S_2})(\rho g\alpha\overline{\theta s} - \rho g\beta\overline{s^2}) - \frac{1}{2}\rho k\frac{\partial S}{\partial z} - C_{S_1}\rho\frac{\varepsilon}{k}\overline{ws} \tag{4}$$

where

$$\mu_{ef} = \mu + \mu_t \qquad \mu_t = C_\mu f_\mu \rho\frac{k^2}{\varepsilon} \tag{5}$$

The equation set above contains empirical coefficients C_{T_1}, C_{T_2}, C_{S_1}, and $C_{S_{21}}$ as a consequence of modeling the terms involving the fluctuating pressure. The practice introduced by Gibson and Launder (1976) for pure thermal field was adopted and extended to the concentration field by assuming a complete analogy of the physical behaviour between the two scalar fields.

The closure of Equations 3 and 4 requires solution of an additional set of transport equations for turbulence properties, such as the temperature and concentration variances $\overline{\theta^2}$ and $\overline{s^2}$, the correlation between the fluctuating temperature, and concentration $\overline{\theta s}$ and for the turbulence kinetic energy k and its dissipation rate ε. A plausible closed set of equations can be written as follows:

$$\rho \frac{\partial \overline{\theta^2}}{\partial t} = \frac{\partial}{\partial z}\left(\frac{\mu_{ef}}{\sigma_{\overline{\theta^2}}}\frac{\partial \overline{\theta^2}}{\partial z}\right) - 2\rho\overline{w\theta}\frac{\partial T}{\partial z} - \frac{1}{C'_T}\rho\frac{\varepsilon}{k}\overline{\theta^2} \tag{6}$$

$$\rho \frac{\partial \overline{s^2}}{\partial t} = \frac{\partial}{\partial z}\left(\frac{\mu_{ef}}{\sigma_{\overline{s^2}}}\frac{\partial \overline{s^2}}{\partial z}\right) - 2\rho\overline{ws}\frac{\partial S}{\partial z} - \frac{1}{C'_S}\rho\frac{\varepsilon}{k}\overline{s^2} \tag{7}$$

$$\rho \frac{\partial \overline{\theta s}}{\partial t} = \frac{\partial}{\partial z}\left(\frac{\mu_{ef}}{\sigma_{\overline{\theta s}}}\frac{\partial \overline{\theta s}}{\partial z}\right) - \rho\overline{ws}\frac{\partial T}{\partial z} - \rho\overline{w\theta}\frac{\partial S}{\partial z} - \frac{1}{C'_{TS}}\rho\frac{\varepsilon}{k}\overline{\theta s} \tag{8}$$

$$\rho \frac{\partial k}{\partial t} = \frac{\partial}{\partial z}\left(\frac{\mu_{ef}}{\sigma_k}\frac{\partial k}{\partial z}\right) + \rho g(\alpha\overline{w\theta} - \beta\overline{ws}) - \rho\varepsilon \tag{9}$$

$$\rho \frac{\partial \varepsilon}{\partial t} = \frac{\partial}{\partial z}\left(\frac{\mu_{ef}}{\sigma_\varepsilon}\frac{\partial \varepsilon}{\partial z}\right) + \rho g\frac{\varepsilon}{k}(C_{\varepsilon 3}\alpha\overline{w\theta} - C_{\varepsilon 4}\beta\overline{ws}) - C_{\varepsilon 2}f_\varepsilon\rho\frac{\varepsilon\tilde{\varepsilon}}{k} \tag{10}$$

where f_μ and f_ε are the functions of turbulent Reynolds number $\mathrm{Re}_t = \rho k^2/(\mu\varepsilon)$

$$f_\mu = \exp[-3.4/(1 + 0.02\,\mathrm{Re}_t)^2] \qquad f_\varepsilon = 1 - 0.3\exp(-\mathrm{Re}_t^2) \tag{11}$$

and

$$\tilde{\varepsilon} = \varepsilon - \frac{2\mu}{\rho}\left(\frac{\partial k^{1/2}}{\partial z}\right)^2 \tag{12}$$

The formulation of the above closure model implies several assumptions that need further argument. First, attention is drawn to the diffusion terms that are modeled by the conventional effective eddy-diffusivity expression. A more general, invariant expression for the turbulent diffusion can be derived by truncation of the corresponding differential transport equation for triple moments.

$$\overline{\phi\psi u_j} = -C_\phi\frac{k}{\varepsilon}\left(\overline{u_j u_l}\frac{\partial\overline{\phi\psi}}{\partial x_l} + \overline{\phi u_l}\frac{\partial\overline{\psi u_j}}{\partial x_l} + \overline{\psi u_l}\frac{\partial\overline{\phi u_j}}{\partial x_l}\right) \tag{13}$$

where ϕ and ψ may stand for any fluctuating property, θ, s, u_i, $\partial u_i/\partial x_m$, $\partial\theta/\partial x_m$, $\partial s/\partial x_m$, etc. It is noted that the last two terms are not of diffusive nature for the dependent variable $\phi\psi$, but represent additional source terms. In the 1-D case, assuming that $\overline{w^2}\propto k$ and neglecting the last term (or last two terms, depending upon the meaning of the variables ϕ and ψ), expression 13 reduces to the above eddy-diffusivity hypothesis. It should be noted that the transport equations for triple moments also contain buoyancy terms that act as source or sink of triple moments. Although it is recognized that these terms may be of significance in strongly stratified flows, they have been neglected in the present work, in line with the adopted simplification of Equation 13.

The function $f_\mu(\mathrm{Re}_t)$ of Launder and Sharma (1974) is added to ensure a damping of the velocity fluctuations normal to the wall and to the interfacial layer caused by joint molecular and wall/free surface blockage effects, as is usually done in near-wall shear flows. Admittedly, the damping mechanisms are different: close to the bottom wall and to the top free surface, the major (if not the only) damping will come from the wall/surface blockage and pressure reflection; whereas, at the interfacial layer the major effect will be caused by molecular forces. In the present case, we are not much interested in the near-wall region, so the possible inadequacy of f_μ in modeling the blockage effect is not important. The focus of the present analysis is the layer interface where the molecular effects are dominant. It seems, therefore, justified to use an f_μ function expressed in terms of turbulence Reynolds number Re_t, although the form (Equation 1), which was kept for convenience, may not be fully adequate, because it was tuned for near-wall flows where the blockage effect was also present.

Similar arguments apply to the function $f_\varepsilon(\mathrm{Re}_t)$, which was tuned in conjunction with f_μ within the framework of the low-Re number k–ε model to account primarily for viscous effects on the energy decay, both in near-wall and wall-distant flow regions. It should be noted that in fluids with Prandtl numbers very different from unity, both damping functions should include the effects of Pr numbers. In the present case, dealing with water solutions, the use of turbulent Reynolds number alone seems sufficient.

Finally, attention is drawn to the last term in Equations 3, 4, and 6 to 8, which represent the sink of dependent variables. In Equations 6 and 7 these terms replace the scalar dissipation rates ε_θ and ε_s, which could be supplied from separate transport equations. The transport equations for these two variables contain at least twice as many terms as the ε equation. Modeling of various terms in the transport equations for ε_θ and ε_s and determining unavoidable empirical coefficients is burdened with a high uncertainty because of lack of experimental or otherwise available data (e.g., direct numerical simulation [DNS]). The need for these equations was eliminated by adopting constant (and equal) ratios of scalar-to-mechanical time-scales; i.e.,

$$R = \frac{\overline{\theta^2}}{\varepsilon_\theta}\frac{\varepsilon}{2k} = \frac{\overline{s^2}}{\varepsilon_s}\frac{\varepsilon}{2k} = 0.8$$

from which ε_θ and ε_s were deduced. This assumption determines the coefficients $C'_T = C'_S = 1.6$. It should be noted that recent DNS of some simple flows with heat transfer indicated that R varies considerably over the flow domain, especially in flows dominated by buoyancy (e.g., Grözbach and Wörner 1992), but numerical computations of several thermal buoyant flows with the solution of ε_θ-equation and with ε_θ deduced from $R = \text{const}$ show relatively small difference in the reproduction of mean velocity and temperature field (Hanjalić 1994). These findings, together with the mentioned uncertainties in modeling equations for ε_θ and ε_s, as well as a desire to simplify the model to the form that can be used for computation of double-diffusive phenomena in complex geometries, lead to adopting $R = \text{const}$ in the present work.

The sink terms in Equations 3 and 4 originate mainly from the scrambling effect of pressure fluctuations, which tend to isotropize the turbulence field and diminish the correlations between velocity and scalar fluctuations $\overline{w\theta}$ and $\overline{ws}$. Another contribution comes from the molecular dissipation $\varepsilon_{\theta_i} \alpha \overline{(\partial\theta/\partial x_k)(\partial u_i/\partial x_k)}$ and $\varepsilon_{si} \alpha \overline{(\partial s/\partial x_k)(\partial u_i/\partial x_k)}$ of each correlation, respectively. The assumption of local isotropy of the small-scale turbulence at high-Reynolds numbers and away from a solid or free surface implies that ε_{θ_i} and ε_{s_i} are negligible, but, admittedly, they can be important in the region of interfacial layer. A way to account for these effects is to define coefficients C_{T1} and C_{S1} as functions of turbulent Reynolds number and scalar flux anisotropy. In the present work, we have assumed that the low-Re number modifications of equations for ε and k will account for these effects.

Equation 8 contains no pressure term, and the molecular destruction $\varepsilon_{\theta s} \alpha \overline{(\partial\theta/\partial x_k)(\partial s/dx_k)}$ is the only sink of the $\overline{\theta s}$ correlation. For that reason $\varepsilon_{\theta s}$ cannot be neglected, and in the present work, we have modeled this term, as shown in Equation 8. Because of lack of experimental or DNS evidence, this apparent inconsistency cannot be explained at present, except by assumption that the fluctuations in two scalar fields are more correlated in between at small scales, than with the velocity fluctuations.

Model truncation: a two-equation closure

The above equations make a closed set that could be solved numerically for the prescribed geometry and boundary and initial conditions. However, it should be noted that for complex geometries solving the second-moment turbulence models may pose serious computational demands, and the full model may not be suitable for application in more complex situations, except for 1-D or boundary-layer-type flows. Hence, in the present phase of our work, we have confined ourselves to a still simpler form of the model, which is an extended variant of the conventional low-Re number k–ε turbulence model, but upgraded in several respects on the basis of the above listed full second-order model to account for most of the mentioned specific effects. The reason for adopting this model is its suitability for incorporation into generally available three-dimensional (3-D) numerical codes for solving the Navier–Stokes equation in more complex situations, such as those in real engineering or natural systems.

The model used here solves the mean energy and concentration Equations 1 and 2, but closure is accomplished by the standard form of gradient expressions for turbulence fluxes of heat and species:

$$\overline{w\theta} = -\frac{\mu_t}{\rho\sigma_T^t}\frac{\partial T}{\partial z} \qquad \overline{ws} = -\frac{\mu_t}{\rho\sigma_S^t}\frac{\partial S}{\partial z} \tag{14}$$

In this way, we have eliminated the need to solve Equations 3, 4, and 6–8, and have solved only Equations 9 and 10, which supplied k and ε, used to specify the turbulent viscosity coefficient μ_t and to define the turbulence time-scale $\tau = k/\varepsilon$. However, in order to eliminate the mentioned deficiency of the gradient transport hypothesis, implied by Equations 14, corrective buoyancy parameters have been introduced, by extending to the concentration field the approach introduced by Gibson and Launder (1976) for the thermal buoyant field. This method first involves the truncation of the full differential transport equations for turbulent fluxes of heat and species $\overline{w\theta}$ and $\overline{ws}$, respectively, into an algebraic expression for these quantities. This is accomplished by eliminating the differential terms (the difference between the mean-flow convection and total diffusion of fluxes). The algebraic expressions can be reduced further to the form of Equations 14, in which the turbulent Prandtl–Schmidt numbers σ_T^t and σ_S^t become variable in terms of the thermal and species "buoyancy parameters," B_T and B_S, respectively, i.e.:

$$\sigma_T^t = \frac{\Phi}{\Phi_T}\frac{1 + \Phi'_T(C'_T - \Phi_T)B_T - \Phi'_T C'_T B_S}{1 + \Phi(\Phi_T B_T - \Phi_S B_S)} \tag{15}$$

$$\sigma_S^t = \frac{\Phi}{\Phi_S}\frac{1 + \Phi'_S(C'_S - \Phi_S)B_S - \Phi'_S C'_T B_T}{1 + \Phi(\Phi_T B_T - \Phi_S B_S)} \tag{16}$$

where

$$B_T = g\alpha\left(\frac{k}{\varepsilon}\right)^2\frac{\partial T}{\partial z} \qquad B_S = -g\beta\left(\frac{k}{\varepsilon}\right)^2\frac{\partial S}{\partial z} \tag{17}$$

and Φ, Φ_T, Φ'_T, Φ_S, and Φ'_S are the additional empirical coefficients specified in Table 1. It should be noted that all the coefficients in the equations describing the thermal field have been optimized earlier with reference to pure thermal convection (e.g., Hanjalić and Vasić 1993). Because of the scarcity of experimental or DNS data for isothermal flows driven by mass buoyancy by unstable concentration stratification, the coefficients in the concentration equations could not be determined independently. It was expected that a full analogy would exist between the two scalar fields, save for Prandtl–Schmidt numbers. However, an attempt to use the same coefficients in analogue terms in the species concentration equations resulted in acceptable agreement with experiments for some cases considered, but failed to reproduce those at the edge of stability of the interfacial layer, resulting invariably in the flow laminarization. Better results were achieved by adjusting the coefficient C_{S2} to 0.9 (as compared with $C_{T2} = 0.6$). In addition, the coefficient with the new source term in the dissipation equation $C_{\varepsilon 4}$, was determined on

the basis of testing the present model against a double-diffusive experiments described later.

Although expressions 14 imply, at first glance, that the turbulent fluxes will tend to zero if the mean profiles of temperature and concentration are close to uniform, it should be pointed out that these gradients appear both in the nominators and denominators of the expressions for σ_T^t and σ_S^t. Hence, even small values of these gradients make a sufficient contribution and substantially increase the turbulent exchange coefficient μ_t and, as shown later, secure reasonably good predictions of both the temperature and concentration field in the mixed layers.

The coefficients in the equations have the following values (in addition to the standard coefficients for the isothermal flows) $C_\mu = 0.09$, $C_{\varepsilon 1} = 1.44$, $C_{\varepsilon 2} = 1.92$ and $\sigma_\varepsilon = 1.3$ (Table 1).

Numerical method

The modeled equation set was solved numerically using a general two-dimensional finite-volume Navier–Stokes code, which was adapted for 1-D unsteady computation. A collocated numerical grid was used for all variables with typically 100 grid points clustered around the layer interface and close to the bottom wall and free surface. A first-order, fully implicit scheme was applied for time marching, with the starting step roughly one order of magnitude smaller than the Brunt–Väilsäla frequency of the system. A second-order accurate central differencing scheme was used for the discretization of the diffusion terms. Depending upon the boundary conditions, in some cases the time-step was increased in the course of computations. Typically, several thousand time integrations were needed to cover the field evolution of laboratory experiments considered, but most of the runs took less than a few hours (and some considerably less) on a Hewlett–Packard 715 workstation.

Results and Discussion

To demonstrate the predictive ability of the model proposed, and to optimize the new coefficient $C_{\varepsilon 4}$, we have selected the experimental results of Bergman et al. (1985b), in which an initially isothermal, almost linear, salt-stratified, 180-mm deep water solution, placed in a square container, was heated from below. The initial stratification was achieved by filling the container with several layers of solutions of different concentrations (in decreasing salinity from bottom to top) and left for a few days until the molecular diffusion smoothed from step-like concentration profile into an almost linear one.

Heat supplied at the bottom will cause unstable stratification in the lower layer that will be opposed by the stable salt concentration gradient. Therefore, the stability and growth of the mixed layer that is formed will depend upon the ratio of the heat flux q and the concentration gradient $\partial S/\partial z$. Bergman et al. (1985b, 1986) defined a nondimensional stability parameter as

$$X = \frac{\mathrm{Ra}_T}{\mathrm{Ra}_S} = \frac{\alpha q_b}{\lambda \beta (\partial S/\partial z)} \tag{18}$$

and performed a series of experiments for different values of X. Here Ra_T and Ra_S are the temperature and concentration Rayleigh numbers. (Turner (1965, 1968) used the ratio of density difference across the diffusive interface caused by salinity and temperature, $R_s = \beta \Delta S/(\alpha \Delta T)$ as a stability parameter.) We have selected three different experiments (Nos. 2, 5, and 7) corresponding to values of X of 0.112, 0.369, and 0.825. The corresponding concentration gradients are −19.1, −5.8, and −29.3%/m, and the bottom heat flux $q_b = 40$, 40, and 450 W/m^2, respectively. These three experiments are representative combinations of the two dominant external parameters, X and q, which govern a double diffusive system.

Table 1 Summary of coefficients

$C_{\varepsilon 3}$	$C_{\varepsilon 4}$	$C'_T = C'_S$	$C_{T1} = C_{S1}$	C_{T2}	C_{S2}	Φ	$\Phi_T = \Phi_S$	$\Phi'_T = \Phi'_S$
0.8	1.2	1.6	3.2	0.6	0.9	0.22	0.33	0.155

The first integral properties to be discussed illustrate the dynamics of the growth of the bottom mixed layer. We first consider the variation of the layer thickness h (mm) with time τ for three different values of the stability parameters. After presenting data in $h^2 - \tau$ plot it, was found that for all three considered cases, both the experiments and the predictions follow a quadratic relationship of the following form:

$$h^2 = K(X)\tau + b \tag{19}$$

As might be expected, the mixed layer grows faster in time with an increase in the bottom heat flux or with a decrease in the concentration gradient. Hence, the slope of each individual curve increases with the stability parameter X, and, as seen in Figure 2, this relationship is almost linear, so that h^2/X plotted against time collapses almost into one line, (except for some experimental and computational scatter). This finding confirms the earlier theory of the mixed-layer growth of Turner (1968), which was partially substantiated by his own experiments. The constant b in the equation has a small value, and its appearance is probably a consequence of incomplete adequacy of the form of relationship 19. The present predictions agree particularly well for the two experiments with small stability parameter; whereas, in the case of experiment No. 7, where the stability parameter is close to its upper limit, the agreement is somewhat poorer. Still, the overall agreement might be regarded as satisfactory.

Figure 3 shows the variation of the temperature (not normalized) in the mixed layer against time. Again, both the experiments and predictions follow a similar (quadratic) dependence, $\Delta T_m^2 \propto \tau$, but the agreement between the measured and predicted slopes is satisfactory only for experiment No. 5, which corresponds to the minimum concentration gradient considered. The disagreement can be attributed to several factors, first to the inadequacy of the employed model and to the treatment of the bottom boundary conditions. However, the disagreement in Figure 3 is perhaps overemphasized by the way the data are plotted and attributable to the fine resolution of the quadratic

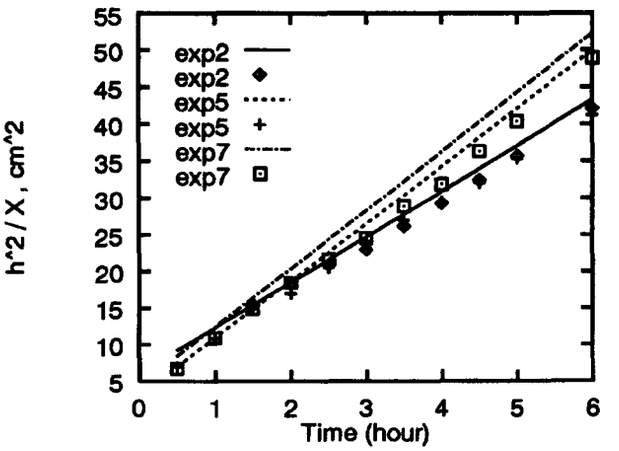

Figure 2 Time-evolution of the mixed-layer height; symbols: measurements Bergman et al. (1985b), lines:

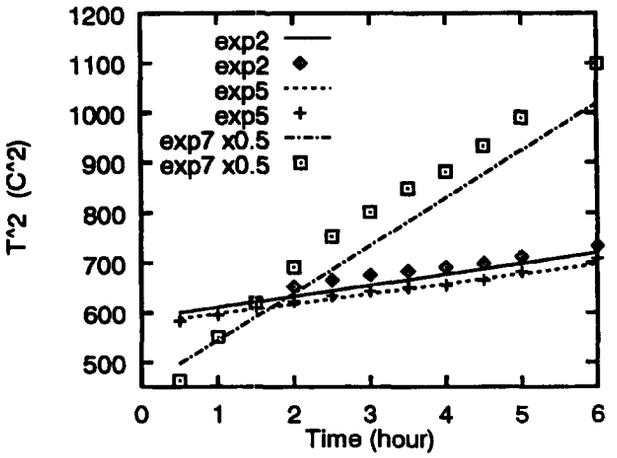

Figure 3 Time-evolution of the mixed-layer temperature; symbols: measurements Bergman et al. (1985b), lines:

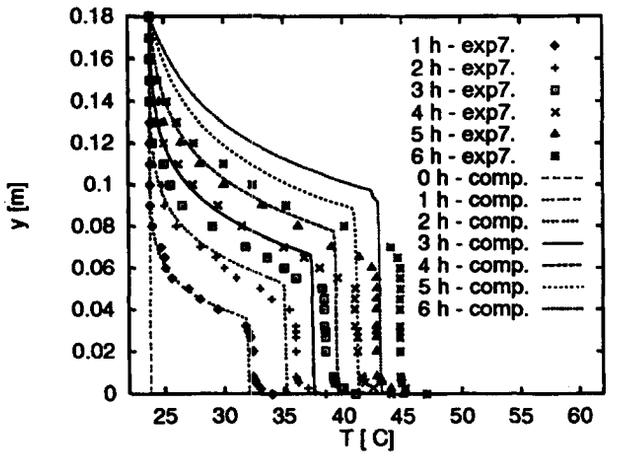

Figure 4 Time-evolution of the mixed-layer temperature; symbols: measurements Bergman et al. (1985b), lines:

temperature scale. As can be seen in Figure 4, comparison of the evolution of temperature profiles in time shows much better agreement. Analogous plots of the evolution of the concentrations in the mixed layer is not presented, because the paper cited did not present measured data. However, in those cases, the model also gave a quadratic form of relationship; i.e., $S_m^2 \propto \tau$, as found by Turner (1968).

We turn now to another set of experimental data of Bergman et al. (1985a). An initial, step-like salinity profile with bottom layer of uniform salinity topped by a fresh water layer of equal depth was left for 26 hours to diffuse molecularly, and then subjected to bottom heating with a uniform heat flux of 500 (W/m^2). Figure 5 shows the evolution of the concentration profiles in time caused by the molecular diffusion. The experimental curve for $\tau = 26$ (h) agrees well with computation, as would be expected, because only molecular transport occurs. However, the more important findings are displayed in Figures 6 and 7, which show computed temperature and concentration profiles at several subsequent time instants when the transport in the bottom layer becomes fully turbulent. Again, for comparison, experimentally obtained curves for $\tau = 5$ h (after the onset of heating) were plotted on both graphs showing reasonable agreement (note a fine resolution of the temperature and concentration scales), demonstrating that the model employed could be

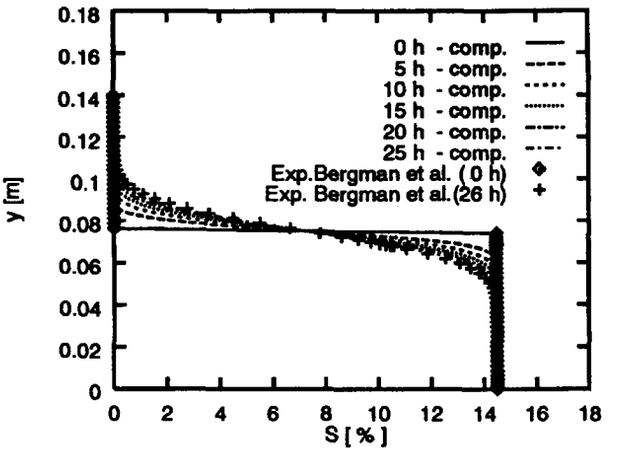

Figure 5 Salinity profiles during the molecular diffusion period; symbols: measurements Bergman et al. (1985a),

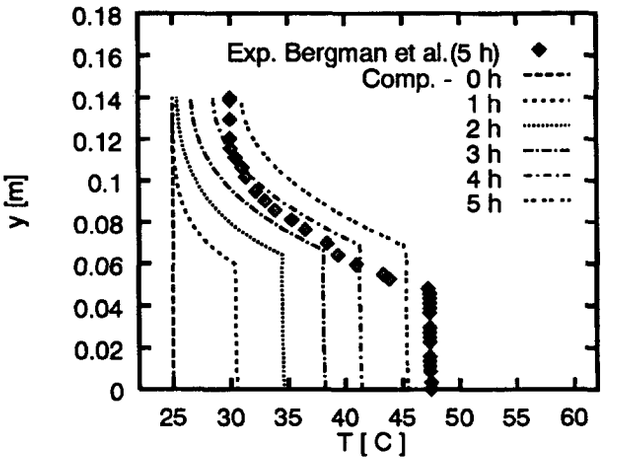

Figure 6 Time-evolution of the temperature profiles after the onset of heating, symbols: measurements Bergman et al. (1985a) lines: predictions

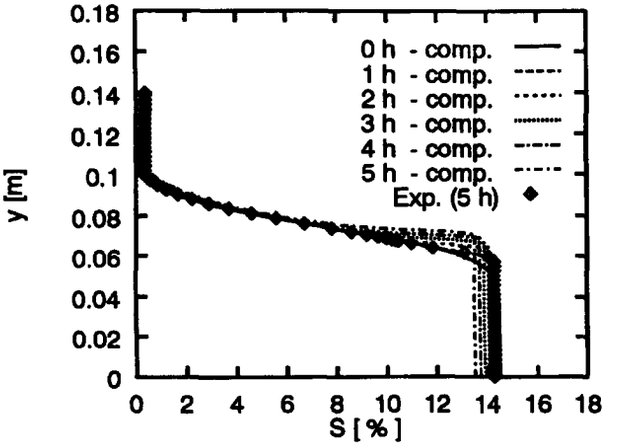

Figure 7 Time-evolution of the salinity profiles after the onset of heating, symbols: measurements Bergman et al. (1985a), lines: predictions

regarded as satisfactory. Unlike the thermal field, to which heat is continuously supplied from below, the concentration field is fully conservative, so that changes in the concentration level in the mixed layer are obviously much smaller than changes in the temperature level. This says nothing, however, about possible differences in the thermal and salinity structure that may exist, but are intractable with single-point statistical models. The apparently faster diffusion of energy into the upper nonturbulent layer than the diffusion of salinity does not have much to do with possible deficiencies in the model but reflects only a substantial difference in the molecular diffusivity of the thermal and concentration fields.

Finally, we consider a case with two fully turbulent mixed layers separated by a sharp diffusive interface, as explored experimentally in the pioneering work of Turner (1965). In contrast with the previous case, both the upper and lower layers are made turbulent by mechanical stirring, (this was repeated during the experiment until the convection in the upper layer was established), while the interface was artificially maintained for a period of time by inserting a thin sheet between the layers.

To simulate such an experiment, we started computations with high levels of turbulence in each layer, but artificially fixed zero value for the turbulent kinetic energy at the midpoint of the diffusive interface (this restriction was removed after the process evolved for some time). The computations, carried out for a series of different initial density differences between the two layers, showed expected behaviour, as can be seen from a sample of results presented in Figures 8 to 10, where the profiles of temperature, concentration, and turbulence Reynolds number at different time instants are plotted.

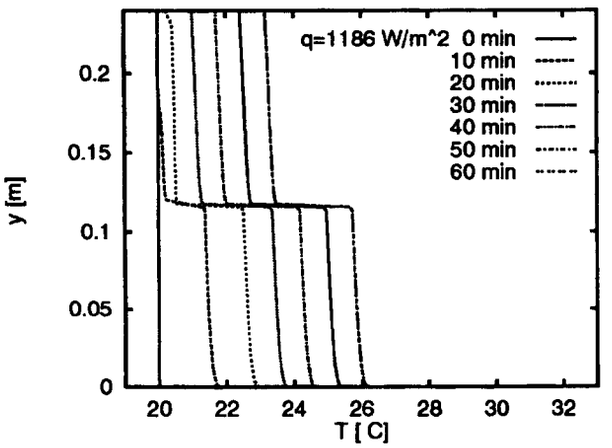

Figure 8 Time-evolution of the temperature field in a double mixed-layer pond

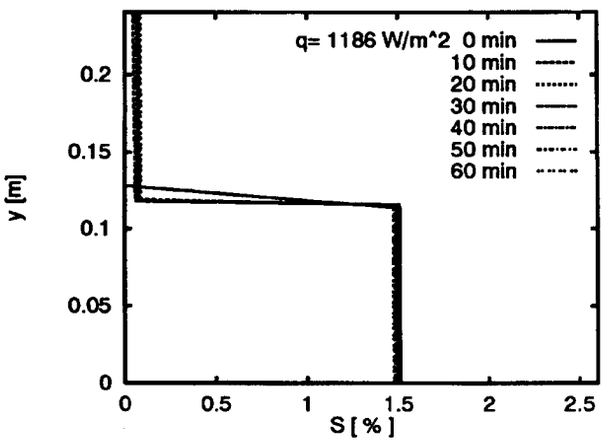

Figure 9 Time-evolution of the salinity field in a double mixed-layer pond

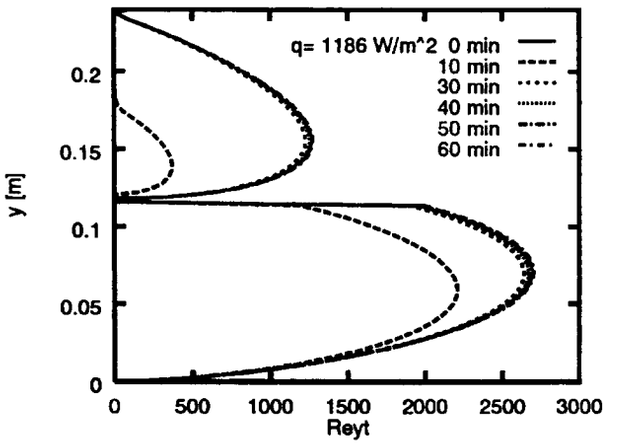

Figure 10 Predicted distribution of the turbulence Re_t number in a double mixed-layer pond

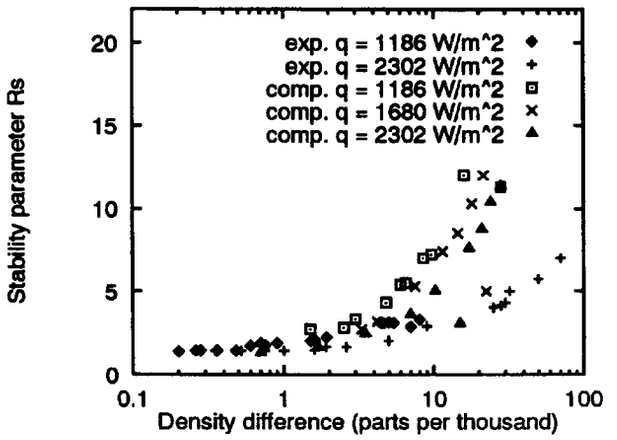

Figure 11 Turner's stability parameter against the net density difference, experiments Turner (1968)

No detailed experimental data are available for comparison. However, to illustrate the broad agreement with measurements, in Figure 11, we compare Turner's stability parameter (the ratio of density differences attributable to salinity and temperature) $R_s = \beta\Delta S/\alpha\Delta T$ *versus* the total density difference $\Delta\rho = \alpha\,\Delta T + \beta\,\Delta S$ for a number of computed cases with experimental data. Despite the large scatter, there is reasonable agreement between the predicted and measured correlation, especially at small stratification.

Conclusions

A modified version of the eddy-diffusivity k–ε, low-Re number turbulence model with *variable* turbulent Prandtl–Schmidt numbers for heat and species in terms of buoyancy parameters B_T and B_S has been derived by truncating the modeled differential transport equations for turbulent fluxes of heat and species. The model yields broadly satisfactory predictions of the time evolution of temperature, concentration, density, and turbulence field, as well as the dynamics of some integral properties in several

cases of double-diffusive salt-stratified ponds subjected to bottom heating. The model also reproduces the time evolution of the integral properties (height of the bottom mixed layer and its bulk mean temperature and concentration) in accordance with the general relationships introduced earlier by Turner (1965, 1968).

Admittedly, the model has many empirical coefficients, which are unavoidable, because many terms in the transport equations must be modeled. The coefficients in the equations for mechanical and thermal turbulence properties initially were taken over from earlier studies of flows dominated purely by thermal buoyancy. The expectation that complete equivalence should exist between the set of coefficients for the two scalar fields, (temperature and concentration) was not fulfilled, however, at least within the framework of the two-equation model adopted. Optimum agreement for all the considered test cases was achieved only after two of the coefficients in the equation for the concentration flux were re-adjusted. Further studies and model calibrations are needed, preferably of systems dominated solely by concentration buoyancy, to clarify possible differences between the buoyant thermal and concentration fields, for which new experimental or DNS data are required. Also, better insight into the effects of mixed terms, particularly of the double-scalar correlation $\overline{\theta s}$ is needed before a more general model for double-diffusive systems can be designed.

References

Bergman, T. L., Incropera, F. P. and Stevenson, W. H. (1985a). *Rev. Sci. Instrum.*, **52**, 291–296

Bergman, T. L., Incropera, F. P. and Viskanta, R. (1985b). A differential model for salt-stratified, double-diffusive systems heated from below. *Int. J. Heat Mass Transfer*, **28**, 779–788

Bergman, T. L., Incropera, F. P. and Viskanta, R. (1986). Correlation of mixed layer growth in a double-diffusive, salt-stratified system heated from below. *J. Heat Transfer*, **108**, 206–211

Fernando, H. J. S. (1989). Buoyancy transfer across a diffusive interface. *J. Fluid Mech.*, **209**, 1–34

Gibson, M. M. and Launder, B. E. (1976). On the calculation of horizontal, turbulent, free shear flows under gravitational influence. *J. Heat Transfer*, **98C**, 81–87

Grözbach, G. and Wörner, M. (1992). Analysis of second-order transport equations by numerical simulations of turbulent convection in liquid metals. *Proc. 5th International Topical Meeting on Nuclear Reactor Thermal Hydraulics, NURETH-5*, (Salt Lake City, UT), Vol. II., 358–365

Hanjalić, K. (1994). Achievements and limitations in modeling and computation of buoyant turbulent flows and heat transfer, Special Keynote Lecture, SK-1. *Proc. 10th International Heat Transfer Conference*, G. F. Hewitt et al. (eds.). I. Chem. Engnrs./Taylor and Fransis Inc., Ragby, UK/Bristol, PA, USA, 1–18

Hanjalić, K. and Vasić, S. (1993). Some further exploration of turbulence models for buoyancy driven flows. In *Turbulent Shear Flows*, Vol. **8**, Durst F. et al. (eds.), Springer, Berlin, 319–341

Launder, B. E. and Sharma, B. I. (1974). Application of energy-dissipation model of turbulence to the calculation of flow near a spinning disc. *Lett. Heat Mass Transfer*, **1**, 131

Turner, J. S. (1965). The coupled turbulent transport of salt and heat across a sharp density interface. *Int. J. Heat Mass Transfer*, **8**, 759–767

Turner, J. S. (1968). The influence of molecular diffusivity on turbulent entrainment across a density interface. *J. Fluid Mech.*, **33**, 183–200